Chemistry–A European Journal
Research Article
doi.org/10.1002/chem.202400504
Chemistry Europe
European Chemical Societies Publishing
www.chemeurj.org

Supramolecular Control of the Temperature Responsiveness of Fluorescent Macrocyclic Molecular Rotamers

Stuart N. Berry,[a] Meijun Zou,[a] Sarah L. Nguyen,[a] Aidan E. Sajowitz,[a] Lei Qin,[a] William Lewis,[a, b] and Katrina A. Jolliffe*[a, c, d]

To fully harness the potential of molecular machines, it is crucial to develop methods by which to exert control over their speed of motion through the application of external stimuli. A conformationally strained macrocyclic fluorescent rotamer, **CarROT**, displays a reproducible and linear fluorescence decrease towards temperature over the physiological temperature range. Through the external addition of anions, cations or through deprotonation, the compound can access four discreet rotational speeds *via* supramolecular interactions (very slow, slow, fast and very fast) which in turn stop, reduce or enhance the thermoluminescent properties due to increasing or decreasing non-radiative decay processes, thereby providing a means to externally control the temperature sensitivity of the system. Through comparison with analogues with a higher degree of conformational freedom, the high thermosensitivity of **CarROT** over the physiological temperature range was determined to be due to conformational strain, which causes a high energy barrier to rotation over this range. Analogues with a higher degree of conformational freedom display lower sensitivities towards temperature over the same temperature range. This study provides an example of an information rich small molecule, in which programable rotational speed states can be observed with facile read-out.

Introduction

The ability to control molecular motion through the application of external stimuli is key to the development of nanoscale machinery with sophisticated functions. While considerable effort has been employed to develop molecular machinery for which the addition of an external analyte regulates the speed and/or direction of molecular motion, rather than simply providing an on/off response, one of the current limitations of nanoscale machines is the limited ability to control their speed.[1–16] Exploiting the potential of these nanoscale systems to provide macroscopic outputs or work (i.e. some kind of function) presents a further challenge.[17]

Changes in the rate of molecular motion can be directly used for sensing temperature[18–20] and/or viscosity[21,22] with numerous potential biological[23,24] and industrial applications.[25–27] If molecules are suitably designed, higher temperature or lower viscosities can lead to increased molecular motion resulting in increased non-radiative 'dark' decay from the excited state and hence thermoresponsive changes in fluorescence.[28,29] There are many examples of fluorescent molecules that respond to temperature (i.e. molecular thermometers); these can be ratiometric,[30–34] function over a range of temperatures[30,35] use lifetime[36] or intensity-based read-outs and can be composed of small organic molecules,[18,37–39] metal-complexes,[35,40–42] quantum dots,[43–45] and polymeric materials[46–48] among others. Recent focus has been on the design of molecular thermometers with increased temperature sensitivity[34] over different temperature ranges,[27] or targeting to specific cellular organelles.[49,50] However, modulation of the response of molecular thermometers to temperature through application of an external stimulus has not yet been investigated.

Despite the many examples of small molecule fluorescent molecular thermometers, the rules that govern the design of a highly sensitive thermometer, particularly over the physiological temperature range (20 °C–40 °C) are unclear. Furthermore,

[a] *Dr. S. N. Berry, M. Zou, S. L. Nguyen, A. E. Sajowitz, Dr. L. Qin, Dr. W. Lewis, Prof. K. A. Jolliffe*
School of Chemistry
The University of Sydney
NSW, 2006, Australia
E-mail: kate.jolliffe@sydney.edu.au
[b] *Dr. W. Lewis*
Sydney Analytical
The University of Sydney
NSW, 2006, Australia
[c] *Prof. K. A. Jolliffe*
The University of Sydney Nano Institute (Sydney Nano)
The University of Sydney
NSW, 2006, Australia
[d] *Prof. K. A. Jolliffe*
Australian Research Council Centre of Excellence for Innovations in Peptide and Protein Science
The University of Sydney
NSW, 2006, Australia

Supporting information for this article is available on the WWW under https://doi.org/10.1002/chem.202400504Supporting information for this article is available on the WWW under https://doi.org/10.1002/chem.202400504

despite several studies on the molecular motion of macrocycles in solution,[51–53] very few macrocyclic fluorescent thermometers have been developed.[33,35] Since it is well established that the conformations of macrocyclic systems can be controlled through ion-binding,[15,17,54] these seem ideal systems for the development of controllable and thermoresponsive molecular motion.

Here we investigate how the rotational speed of fluorescent macrocycles containing both cation and anion binding sites can be altered via binding of ions and by deprotonation, resulting in changes in the thermosensitivity of these molecules. We reveal that four different rotational speeds (very fast, fast, slow and stopped) can be accessed *via* supramolecular control. In addition, through the synthesis and evaluation of structurally related analogues with inherently different energy barriers to rotation, further insights into how to prepare a molecule with a sensitive thermoresponse for the desired temperature range are uncovered.

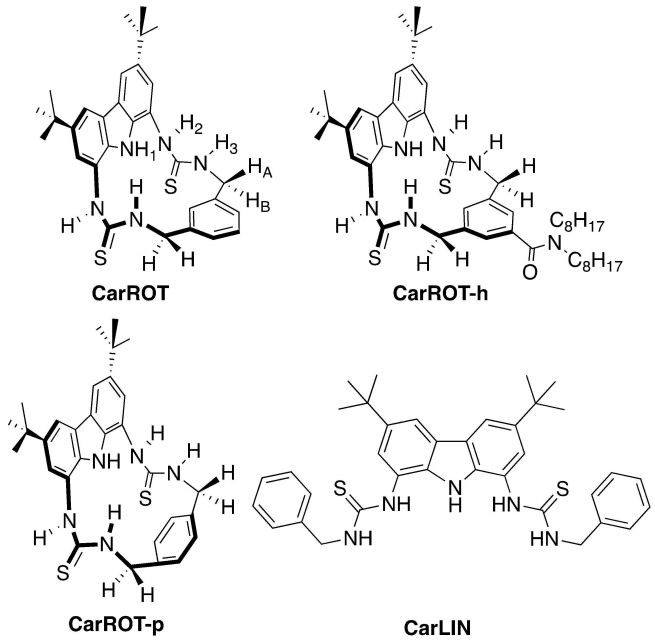

Figure 1. Carbazole rotamers (**CarROTs**) used in this study.

Results and Discussion

The **CarROT** macrocycles (Figure 1) were initially prepared as analogues of recently reported fluorescent macrocyclic receptors for dicarboxylate anions[55] and comprise a 1,8-diaminocarbazole fluorophore bearing two thiourea groups, cyclised using either a 1,3-xylyl (**CarROT** and **CarROT-h**) or a 1,4-xylyl spacer (**CarROT-p**). **CarLIN**[55] is a linear analogue of the macrocycles and consists of a bis-thiourea flanked by two benzyl groups. We first prepared **CarROT** by reaction of carbazole 1,8-diisothiocyanate with 1,3-diaminoxylene and obtained the desired macrocycle in moderate yield (45%). (See ESI for full synthesis details and characterisation data).

Broadening of a number of signals in the ^{1}H and the ^{13}C NMR spectra of **CarROT** suggested the presence of slowly interconverting conformers. Further evidence for the presence of conformers of **CarROT** was obtained by single crystal X-ray crystallography of two sets of crystals of **CarROT** obtained from either methanol or DMF solvents. The two crystal structures (shown overlaid in Figure 2a; further information in ESI section 4.4) differ in the relative orientation of the xylyl-phenyl rings, which are orientated either 'up' or 'down' with respect to the carbazole, suggesting that while the macrocycle is conformationally strained due to the limited conformations the 1,3-xylyl-bis thiourea can take, the macrocycle is also flexible enough for the phenyl ring to oscillate through a number of different conformations. In both crystal structures, the carbazole unit is orientated on average at a 93.1° to the thiourea unit ($N_{ali\ thio}$-$N_{ar\ thio}$-C_{carb} angle; average of 6 measurements across all crystal structures obtained) and both thioureas adopt approximately *anti-*, *syn-* conformations, with the thiocarbonyls projecting away from the carbazole units.

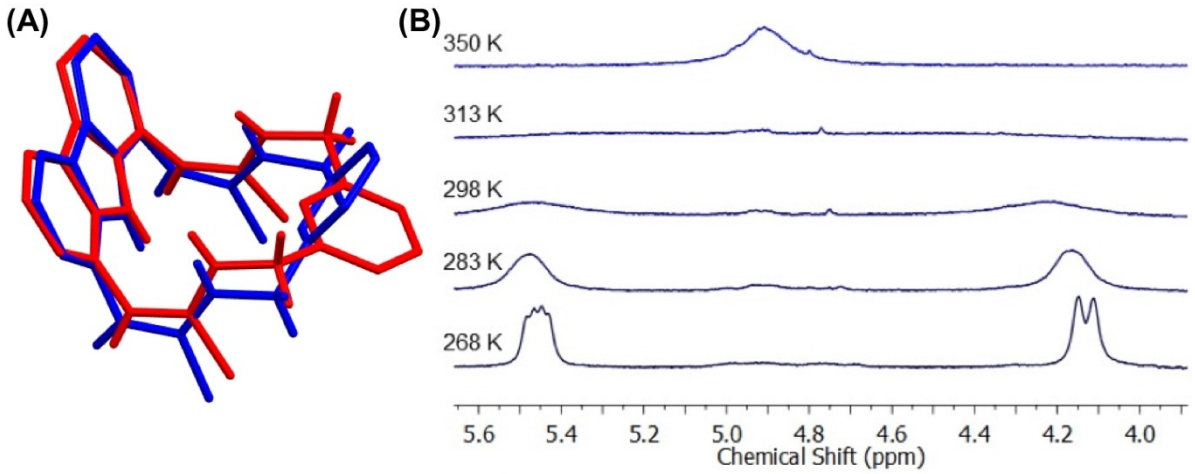

Figure 2. (a) Overlay of two single X-Ray crystal structures obtained for **CarROT** showing multiple conformations of the phenyl ring. (b) Effect of temperature on the methylene region of the ^{1}H NMR spectra of **CarROT**. Partial ^{1}H NMR spectra of **CarROT** showing protons H_A and H_B in DMF-d_7 at various temperatures.

Given the isolation of different conformers of **CarROT** in the solid state, we investigated the conformational flexibility of **CarROT** in solution using variable temperature (VT) NMR studies (Figure 2b and ESI Figure S46–S47) in dimethylformamide-d_7. DMF-d_7 was chosen for its wide temperature range and suitable solubility of the receptor at concentrations required for NMR experiments. The methylene protons (H_A and H_B) on **CarROT** provide an excellent moiety to study molecular motion on the NMR timescale. In DMF-d_7 at 298 K, the signals corresponding to the methylene protons appear very broadened (see ESI Figure S46–S47 for full spectra) suggesting the four protons exist in two chemically inequivalent environments which exchange intermediately on the NMR timescale. As the solution is warmed, the proton signals coalesce at 328 K, which is defined as T_c (coalescence temperature). Furthermore, as the solution is cooled to 268 K no chemical exchange is observed and the proton signals are chemically inequivalent. Line shape analysis[56] was performed in order to estimate the rate constant of exchange and therefore quantify the temperature dependence on molecular motion of the compound (see ESI section 7.2 for details). At 298 K, the rate of exchange constant k was estimated to be 151.02 s^{-1} and at T_c (328 K), $k = 901.04\ s^{-1}$. Fitting the estimated rate constants to the Eyring equation allows the thermodynamic parameters to exchange to be determined: $\Delta H^{\ddagger} = 74.9$ KJ mol^{-1}, $\Delta S^{\ddagger} = 48.2$ J mol^{-1} K^{-1} and $\Delta G_{298K}^{\ddagger} = 60.6$ KJ mol^{-1}.

The absence of any intramolecular H-bonding interactions in the crystal structures of **CarROT** suggests that the restricted rotation observed in solution is a result of steric factors in this strained macrocycle rather than the result of stabilisation of a particular conformation through intramolecular H-bonding, as has been observed previously for small amide-containing macrocycles.[52] Further evidence for this hypothesis was obtained using a combination of ^{1}H NMR experiments. Firstly, a comparison of the chemical shifts of the NH protons of **CarROT** in solvents of differing polarity showed that these varied greatly (ESI Table S5), indicating that these protons are significantly exposed to solvent. Similarly, only very small differences in the rate of deuterium exchange were observed when D_2O was titrated into a solution of **CarROT** in either acetone-d_6 or acetone-d_6 (1% added H_2O) (ESI Figure S55 and S56), again suggesting that no intramolecular hydrogen bond interactions are present. Finally, the chemical shifts of the NH protons exhibited a large temperature dependence in DMF-d_7 [$\Delta\delta$(NH)/ΔT = −20.6, −4.9 and −1.9 ppb/K for the carbazole NH, aromatic and aliphatic thiourea protons, respectively, all of which lie in the expected range for a non-hydrogen bonded proton.[57]

Next, the fluorescence spectra of **CarROT** at different temperatures within the physiological temperature range were measured in CH_3CN. Upon excitation at 295 nm at 20 °C, the fluorescence spectrum of **CarROT** exhibited two emission maxima ($\lambda_{em\ max}$) at 360 nm and 377 nm. After warming the solution to 40 °C the emission spectrum of **CarROT** was significantly quenched (approx 47% quenching) (Figure 3a). Measuring the emission spectra in two degree increments between 20 °C and 40 °C revealed that maximal intensity decreased in linear manner with temperature (Figure 3b). The temperature sensitivity was calculated by taking the gradient of the linear fit at 360 nm between 20 °C and 40 °C (details in the ESI section 5.2) and **CarROT** was determined to have a high temperature sensitivity with fluorescence intensity decreasing by 2.31%/°C. Furthermore, when the compound was subjected to five heating and cooling cycles between 20 °C and 40 °C

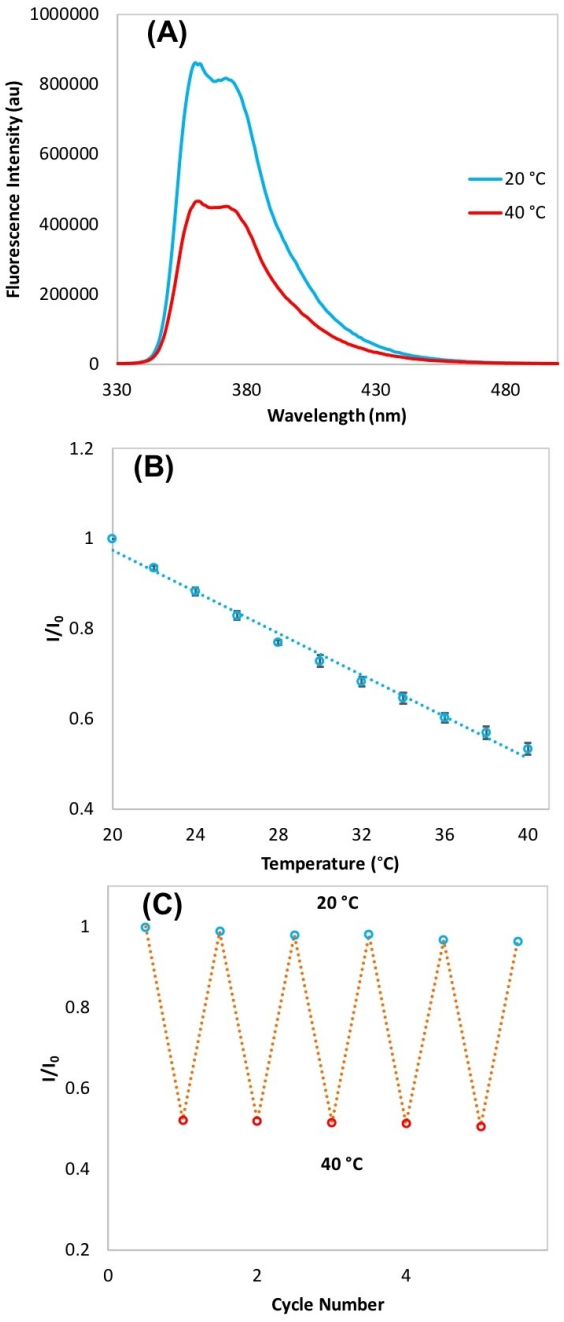

Figure 3. (a) Fluorescence spectra of **CarROT** (25 μM) in CH_3CN at 20 °C and 40 °C, $\lambda_{ex} = 295$ nm. (b) Temperature dependence on normalized maximal fluorescence ($\lambda_{ex\ max} = 360$ nm) of **CarROT** (25 μM, CH_3CN) upon heating between 20 °C and 40 °C. Error bars show ± standard deviation from 4 independently repeated experiments. Dotted line represents linear fitting, $R_2 = 0.9908$. (c) Reproducibility of temperature dependence on fluorescence, showing heating and cooling cycles between 20 °C and 40 °C.

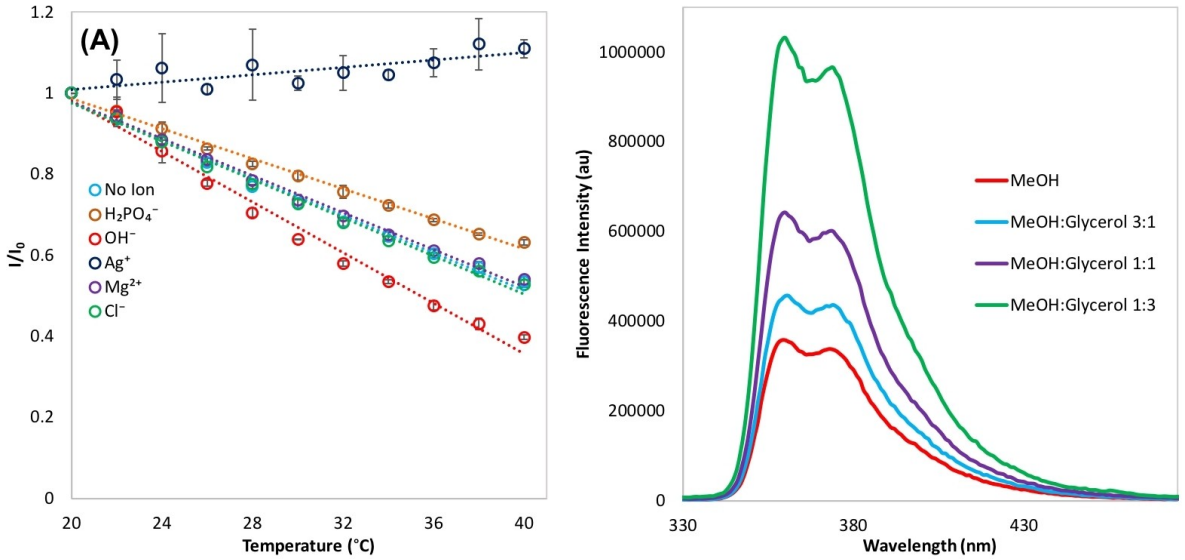

Figure 4. (a) Effect of external ion addition on the fluorescence temperature sensitivity of **CarROT** (25 μM, CH_3CN). Normalised maximal fluorescence intensity at 20 °C versus intensity at the stated temperature, with and without 40 equivalents of stated ion ($\lambda_{em\ max}$ = 360 nm for no ion, Cl^- and Mg^{2+}, $\lambda_{em\ max}$ = 370 nm for Ag^+, $\lambda_{em\ max}$ = 375 nm for $H_2PO_4^-$ and $\lambda_{em\ max}$ = 385 nm for OH^-). Error bars are ± standard deviation, each data point is an average of at least 2 independently repeated experiments. Dotted lines represent linear fittings. (b) Fluorescence spectra of **CarROT** (25 mM) in methanol/glycerol mixtures of varying viscosity at 298 K. λ_{ex} = 295 nm in all cases.

(Figure 3c), maximal fluorescence intensity was found to be remarkably reproducible, suggesting that the linear response to temperature is predictable within this temperature range and that minimal thermo- or photo-degradation is occurring over the time course of the experiment.

The thermo-luminescent properties of **CarROT** arise from increased molecular motion at elevated temperatures that dissipates excited energy as non-radiative vibrational decay. Due to the conformationally strained nature of the macrocycle, we reasoned that motion occurs in a reasonably well-defined manner and this aids in the reproducibility of the fluorescence response. We hypothesised that the binding of an ion to **CarROT** may freeze the conformation of the macrocycle and therefore alter the thermo-luminescent properties. The bis-thiourea macrocycle possesses both anion binding sites (hydrogen bond donating NH's) and cation binding sites (thiocarbonyls), additionally, the macrocycle may be deprotonated creating a charged species which may form an intramolecular hydrogen bond, further altering the macrocycle's conformation and resultingly the thermo-luminescent properties.

The fluorescence spectra at various temperatures between 20 °C and 40 °C were measured in 2 degree increments for **CarROT** (25 μM) in CH_3CN with and without the presence of 40 equivalents of various salts to saturate binding interactions (tetrabutylammonium chloride, tetrabutylammonium dihydrogen phosphate, tetrabutylammonium hydroxide, silver nitrate and magnesium nitrate, Figure 4a). While addition of Cl^- and Mg^{2+} resulted in minimal changes to the fluorescence temperature sensitivity, addition of $H_2PO_4^-$ decreased the thermo-luminescence properties to 1.85 %/°C and addition of Ag^+ caused a slight increase in fluorescence intensity as temperature was warmed to 40 °C but essentially turned off **CarROT's** sensitivity towards temperature changes. Conversely, deprotonation with 40 equivalents of OH^- resulted in an increase in the temperature sensitivity of **CarROT** to 3.12 %/°C. A summary of the fluorescence sensitivity properties of **CarROT** is shown in Table 1 with additional fluorescence spectra in the ESI section 5.3.

To further test the hypothesis that ion binding alters molecular motion, thereby affecting luminescent sensitivity, binding strength was quantified with UV-Vis titrations, initially performed in CH_3CN, as summarised in Table 1. Addition of Cl^- and Mg^{2+} resulted in minimal changes in UV-Vis spectra during the titration, indicating no, or very weak binding (ESI Figures S33–S34). During the titration with $H_2PO_4^-$ in CH_3CN on the other hand, a large spectral decrease accompanied by a

Table 1. Summary of ion binding properties and fluorescence temperature sensitivity of **CarROT**.

Ion[a]	MeCN $K_{a\ 1:1}$ (M^{-1})[b]	DMF $K_{a\ 1:1}$ (M^{-1})[c]	T. Sensitivity (%/°C)[d]
No Ion	–	–	2.31
Cl^-	< 10	n/d	2.38
$H_2PO_4^-$	24000	2400	1.85
Ag^+	n/d[e]	n/d[e]	–[f]
Mg^{2+}	< 10	n/d	2.28
OH^-	Deprot.	Deprot.	3.12

[a] Salts added as: TBACl, $TBAH_2PO_4$, $AgNO_3$, $Mg(NO_3)_2$ ($6H_2O$) and TBAOH. [b] Association constant obtained by UV-Vis titration in MeCN and performing a global fit to a 1:1 binding model. [c] Association constant obtained by UV-Vis titration in DMF and performing a global fit to a 1:1 binding model. [d] Fluorescence temperature sensitivity calculated using equation 1 in CH_3CN (details in ESI section 5.2). [e] Binding too strong to fit accurately to a binding model. [f] No fluorescence temperature sensitivity.

bathochromic shift about the absorbance band at 297 nm was observed, along with the presence of clear isosbestic points (ESI Figure S35). Fitting the titration data to a 1:1 binding model using the *Bindfit* web app[58] gave a high binding affinity (K_a = 24,000 M^{-1}). During the titration with Ag^+, again a large decrease and bathochromic shift in the absorbance band at 297 nm was observed. Furthermore, the changes in absorbance could not be fit accurately to a binding model but saturated after one equivalent of Ag^+ was added (ESI Figure S36), suggestive of strong complex formation. The binding of $H_2PO_4^-$ and Ag^+ towards **CarROT** was also measured in the more competitive dimethylformamide (ESI Figures S38–S39). Here, the binding strength of $H_2PO_4^-$ decreased by an order of magnitude however, the binding with Ag^+ remained too strong to be measured accurately. Titration experiments were also performed with TBA OH (added with a 1% CH_3OH content) in both solvents (ESI Figure S37 and S40). In this case the changes in absorbance spectra were very different with absorbance bands forming at 354 nm, indicative of deprotonation of the carbazole NH proton.[59]

Upon deprotonation of **CarROT** with TBA OH, the thermoluminescence sensitivity increases to 3.12%/°C. Studies have shown that the transition state to intramolecular rotation can be stabilised by inducing formation of an intramolecular hydrogen bond by protonation which reduces steric repulsion, causing more rapid rotations.[10] It is likely that a similar process is occurring here but with deprotonation. The most acidic proton is the central carbazole NH (pK_a = 19.9 in DMSO)[60] which could deprotonate and form an intramolecular hydrogen bond between the negatively charged nitrogen and either of the aromatic thiourea groups. A newly formed intramolecular hydrogen bond may stabilise the rotation about the thiourea groups and cause the increase in thermosensitive properties observed. While we were unable to experimentally confirm the presence of an intramolecular hydrogen bond in the deprotonated form of **CarROT**, DFT calculations at the B3LYP/6-31G* theory level indicate the formation of such a hydrogen bonded interaction is plausible (Figure 5f).

To confirm that the fluorescence intensity of **CarROT** is affected by restriction of molecular motion, fluorescence spectra were obtained in methanol/glycerol mixtures of varying glycerol content at 298 K (Figure 4b). In 1:3 methanol:glycerol, the fluorescence intensity of **CarROT** is approximately three times the intensity than in methanol alone, with intensity decreasing as glycerol content is decreased. The fluorescence intensity dependence on solvent viscosity indicates that hindering molecular motion is affecting the fluorescence response, as predicted. This, coupled with the obtained binding data from UV-Vis titrations suggests that $H_2PO_4^-$ and Ag^+ bind to **CarROT** in such a way that vibrational motion and subsequent non-radiative decay from the excited state is hindered, thereby reducing ($H_2PO_4^-$) or stopping completely (Ag^+) the fluorescence response towards temperature of the compound. Cl^- and Mg^{2+}, which don't show measurable binding interactions towards **CarROT** do not alter the temperature sensitivity of the compound.

Information about the rotational movement of **CarROT** upon the binding of ions was also examined with ^1H NMR titration experiments. During the titration with TBA H_2PO_4 in DMF-d_7 at 298 K, both the signals attributable to the thiourea NH protons shift downfield, indicative of hydrogen bonding to the receptor. Furthermore, the carbazole NH proton signal shifts upfield, suggesting it may not be involved in binding to the anion. Considering the NMR binding information, and the conformation based on the crystal structures, an energy minimised binding model to $H_2PO_4^-$ was calculated using DFT, (Figure 5d) wherein the $H_2PO_4^-$ is bound by the four thiourea protons. Fitting the ^1H NMR titration data to a 1:1 binding model provided a moderate binding constant of 300 M^{-1}, which is consistent with, although slightly lower than, that obtained from the UV-Vis titrations (ESI Figure S52). Closer examination of the two methylene proton signals revealed that at low ion

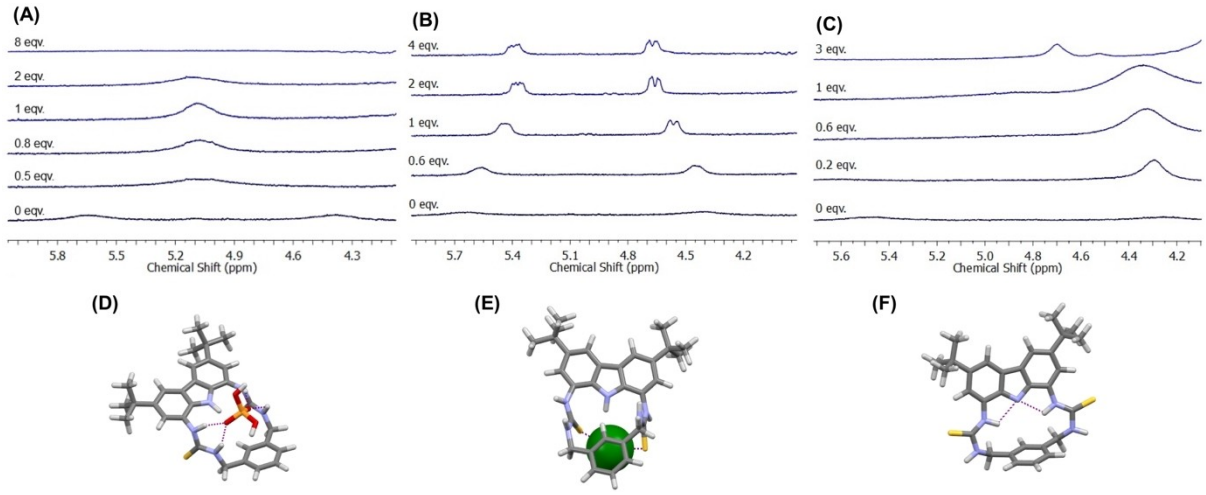

Figure 5. Effect of ion binding on ^1H NMR spectra of **CarROT**. Partial ^1H NMR spectra of **CarROT** in showing the methylene protons (H_A and H_B) in (1.5 mM) DMF-d_7 (a) during the titration with TBA H_2PO_4 at 298 K, (b) during the titration with $AgNO_3$ at 298 K and (c) during the titration with TBA OH at 298 K. Energy minimised calculated structures (DFT, B3LYP/6-31G*, Spartan'14, Wavefunction®) showing likely binding conformations with (d) $H_2PO_4^-$, (e) Ag^+ and (f) after deprotonation with OH^-.

concentrations the methylene proton signals begin to coalesce (Figure 5a). This is indicative of a conformational change which occurs upon binding, bringing the methylene protons into a chemically equivalent environment on the NMR timescale. As binding of the anion occurs reversibly, at low anion concentrations an equilibrium mixture of exchanging bound and unbound receptors is present, which is why the protons coalesce. However, the signals for these protons begin to split when more than one equivalent of anion is added, suggesting that as binding saturates (all receptors bound to an anion on NMR timescale), the conformation of the receptor becomes refrozen on the NMR timescale. This is consistent with the reduced fluorescence temperature sensitivity observed when $H_2PO_4^-$ is added to **CarROT**, suggesting that upon saturation of binding, the receptor is less likely to dissipate excited energy as vibrational movement, as a result of conformational restrictions that are enforced upon binding.

A similar titration experiment was conducted with **CarROT** and $AgNO_3$ in DMF-d_7 (Figure 5b and ESI Figure S53). Here, the initially broadened signals for the methylene protons became progressively sharper as Ag^+ was added. The signals continue to sharpen up to the addition of two equivalents of Ag^+, followed by no further changes. Downfield shifts were observed for the signals attributable to the aromatic protons as up to two equivalents of Ag^+ were added, with no further changes upon addition of further equivalents of Ag^+. While these changes could not be fit to a binding model, the data is indicative of very strong binding to Ag^+, as suggested by the UV-Vis titrations, wherein the conformation of **CarROT** becomes frozen upon addition of sub-stoichiometric equivalents of Ag^+. A proposed energy minimised complex with Ag^+ is shown in Figure 5e wherein the Ag^+ cation is bound between both thiocarbonyl units, consistent with previous reports that demonstrate thioureas bind Ag^+ ions through the thiocarbonyl group.[61,62] Once again, this supports the fluorescence temperature sensitivity study wherein the conformational freezing of **CarROT** by Ag^+ prevents the vibrational dissipation of excited energy and therefore stops the thermo-luminescent sensitivity.

Titration experiments with TBA OH gave significantly different ^{1}H NMR spectra. Upon addition of 0.2 equivalents of OH^-, the signals for the separated methylene protons shift to a new coalesced peak at 4.26 ppm (Figure 5c), this is in stark contrast to the VT experiment and titration experiment with $H_2PO_4^-$ where coalescence occurs at 4.95 ppm, indicative of the formation of a new chemical species. Upon addition of increasing amounts of OH^- the coalesced peak at 4.26 ppm becomes more intense, up to the addition of one equivalent then upon further additions of OH^- the peak broadens then shifts a second time to 4.65 ppm, suggesting a second deprotonation event may occur at high OH^- concentration. Furthermore, the signal attributable to the most acidic proton, the carbazole NH proton at 11.7 ppm broadens then disappears upon OH^- addition (ESI Figure S54), suggesting this is the likely site of deprotonation. A model of the possible deprotonated **CarROT** along with intramolecular hydrogen bond formation is shown in Figure 5f wherein an intramolecular hydrogen bond is formed between the carbazole nitrogen and both aromatic thiourea NH protons. The shift from separated to coalesced proton environments at low equivalents of OH^- suggests an immediate conformational change wherein the two methylene environments become chemically equivalent on the NMR timescale, this also serves as qualitative evidence showing that the energy barrier to exchange has lowered and as such helps explain the thermosensitivity experiments wherein **CarROT** is more thermosensitive in presence of OH^-.

With the discovery of the excellent thermo-luminescent properties of macrocyclic carbazole based rotamer (**CarROT**) (*vide infra*), we designed and synthesized two additional **CarROTs** and a linear analogue (**CarLIN**) in order to thoroughly study the properties that make a sensitive molecular thermometer (Figure 1). Analogues **CarROT-p**, **CarROT-h** and **CarLIN** were prepared in a similar fashion to **CarROT** though reaction of carbazole 1,8-diisothiocyanate with the appropriate amine/diamine.

In order to further understand the molecular properties that influence the thermosensitive response of a **CarROT**, we measured the thermoluminescence properties of **CarROT-p**, **CarROT-h** and **CarLIN** between 20 °C and 40 °C in CH_3CN in analogous experiments to those performed with **CarROT** (Figure 6a and ESI Figure S24–S32), summarised in Table 3). Interestingly, **CarLIN** does not exhibit a luminescent response towards temperature, **CarROT-p** exhibits a reduced response compared to **CarROT** and **CarROT-h** displays an almost identical response to **CarROT**.

All three of these responses can be rationalised. **CarROT** and **CarROT-h** have almost identical thermo-luminescent properties (2.31 %/°C and 2.33 %/°C respectively) which shows that functionalisation at the phenyl ring does not affect the fluorescence quenching at elevated temperatures. This suggests that the increased molecular movement at elevated temperatures is not a 'ring flip' where the phenyl ring could rotate 'through' the macrocycle. The octyl chains on **CarROT-h** would prevent such a flip from occurring and, given the almost identical thermoluminescent properties of the two macrocycles, this suggests neither are able to flip through themselves. Additionally, the two macrocycles are expected to have the same conformation in solution due to them both being linked by a 1,3-xylyl linker, which suggests that the increased motion at high temperatures observed in both molecules is likely to be the same. Taken together with the ^{1}H NMR and crystallographic evidence, we propose the motion occurring is an oscillation wherein the phenyl ring alternates from pointing 'up' and 'down' at increased temperature. This can occur by rotations about the thiourea and methylene linker groups.

CarROT-p showed reduced fluorescence temperature sensitivity (1.41 %/°C) in comparison to **CarROT** and **CarROT-h**. Variable temperature ^{1}H NMR studies with **CarROT-p** in dimethylformamide-d_7 (ESI Figure S48–S49 and summarised in Table 2) showed that at 298 K the signals attributable to the four methylene protons are coalesced to a broad peak. Decoalescence was observed at 254 K and even at 215 K (the lower temperature limit for the solvent) the two proton resonances were not fully resolved, preventing a full line-shape analysis from being conducted. Nonetheless, this indicates a

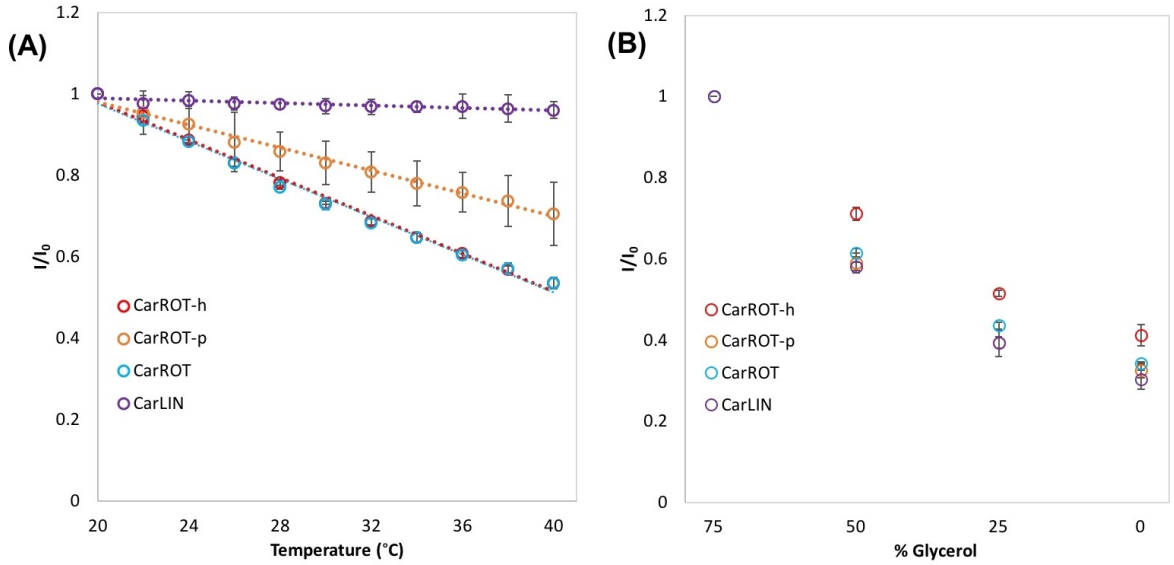

Figure 6. a) Temperature dependence on normalized maximal fluorescence intensity of **CarROT-h, CarROT-p**, **CarROT** and **CarLIN** between 20 °C and 40 °C, 25 μM in CH_3CN. b) Normalised changes in maximal fluorescence intensity of **CarROT-h**, **CarROT-p**, **CarROT** and **CarLIN** in methanol mixtures with differing glycerol content (25 μM). All data is an average of at least 2 independently repeated experiments with error bars ± standard deviation about the mean. Dotted lines are linear fittings. λ_{ex} = 295 nm, $\lambda_{em\ max}$ = 360 nm for all rotamers except **CarLIN**, λ_{ex} = 320 nm, $\lambda_{em\ max}$ = 375 nm.

Table 2. Summary of fluorescence thermo-luminescent and VT NMR properties of **CarROT** analogues.

	T. Sensitivity (%/°C)[a]	T_c (K)[b]
CarROT	2.31	328
CarROT-h	2.33	n/d[c]
CarROT-p	1.41	254
CarLIN	0.0015	< 215[d]

[a] Fluorescence temperature sensitivity calculated using equation 1 (details in ESI section 5.2) in CH_3CN. [b] Coalescence temperature from VT ^{1}H NMR studies in DMF-d_7. [c] not determined due to poor solubility. [d] T_c is lower than the freezing point of the solvent.

significantly lower barrier to exchange (and therefore rotation) than for **CarROT** where the signals attributable to the methylene groups appear separated in this solvent at 298 K (Figure 2b). This lower barrier to exchange arises from the greater conformational freedom in **CarROT-p** as opposed to **CarROT** due to the 1,4-xylyl linker instead of the 1,3-xylyl linker. DFT modelling of **CarROT-p** suggests the compound exists in an almost planar conformation and the central phenyl ring (which is less sterically strained) sits perpendicular to the carbazole unit and can freely rotate about the two methylene units (ESI Figure S57). This conformation is further supported by the significantly downfield shifted signal for the carbazole NH proton (δ = 6.1 ppm) in comparison to that of **CarROT** and **CarLIN** (δ = 10.3 and 10.2 ppm, respectively) in d_6-DMSO, which is consistent with the proposed structure in which the aromatic ring current of the 1,4-substituted phenyl group would result in shielding of this proton.

CarLIN shows almost no fluorescence temperature sensitivity (0.0015 %/°C). VT NMR studies in dimethylformamide-d_7 showed the signal for the four methylene protons exists as a well resolved doublet at 350 K, 298 K and 277 K (J = 5.6 Hz) (ESI Figure S50). At 215 K, the methylene proton signal is broadened slightly, but still coalesced. This indicates, as expected, the energy barrier to rotation about these groups is significantly lower than that in **CarROT** and **CarROT-p** and over the physiological temperature range, there is free rotation about these groups in solution. Furthermore, no changes in the thermosensitivity of **CarLIN** were observed upon addition of 40 equivalents of $H_2PO_4^-$ and Ag^+, despite this receptor displaying strong binding affinities towards these ions, which are similar to those of **CarROT** (determined by UV-Vis titrations; see Table 3 and ESI Figure S41–S45).

Surprisingly, when the fluorescence spectra of the four receptors were measured in methanol/glycerol solutions of various viscosity, the normalised response to changes in viscosity for each compound was determined to be almost identical (Figure 6b and ESI Figure S24–S32). The fluorescence spectra for all compounds were quenched to almost the same relative degree in 100 % methanol solution, with fluorescence intensity increasing a similar amount as glycerol content was

Table 3. Summary of ion binding properties of **CarLIN**.

Ion[a]	$K_{a\ 1:1}$ (M^{-1})[b]
Cl^-	900
$H_2PO_4^-$	27000
Ag^+	1,500,000
Mg^{2+}	< 10

[a] Salts added as: TBACl, $TBAH_2PO_4$, $AgNO_3$, $Mg(NO_3)_2$ ($6H_2O$). [b] Association constant obtained by UV-Vis titration in MeCN and performing a global fit to a 1:1 binding model. See ESI section 6.3 for fitted binding isotherms.

increased. This result suggests that freezing or slowing down molecular motion affects the fluorescence properties of all the **CarROT**s in the same way. The differing responses to temperature therefore are due to the differing rotational energy barriers within the physiological temperature range studied. At 20 °C, **CarLIN** is already rapidly rotating in solution, as determined by ^{1}H NMR studies. This means that small increases in temperature do not have a large effect on the rate of rotation and therefore little effect on the fluorescence emission from the excited stated. **CarROT-p** on the other hand has an intermediate rotational energy barrier at 20 °C and therefore is more affected by changes in temperature within this range. **CarROT** and **CarROT-h** have the highest rotational energy barriers at 20 °C and therefore are most affected by changes in temperature over this temperature range, which is reflected by the highest fluorescence sensitivity towards temperature.

The differing rotational energy barriers arise due to the conformational strain imposed by the xylyl linkers and therefore, the conformational strain imposed on **CarROT** is a key factor in strong temperature sensitivity over the physiological range. The conformational strain likely restricts motion at 298 K, whereas the more flexible **CarROT-p** and much more flexible **CarLIN** are too conformationally free at 298 K to exhibit strong temperature dependence. We hypothesise that the temperature sensitivity of **CarROT-p** would increase at lower temperatures and that of **CarLIN** would increase at very low temperatures.

Conclusions

To summarise, we have developed a conformationally strained macrocyclic fluorescent rotamer, **CarROT** which displays a reproducible, linear response to temperature over the physiological temperature range. Through the external addition of anions, cations or through deprotonation, the compound can access four discreet rotational speeds (very slow, slow, fast and very fast) which in turn stop, reduce or enhance the thermo-luminescent properties due to increase or decrease of non-radiative decay processes. Furthermore, by synthesising related analogues, the thermo-luminescent properties were determined to be due to conformational strain which causes a high energy barrier to rotation over the physiological temperature range, compared to more conformationally free analogues which display lower sensitivities towards temperature over the same temperature range. This study provides an example of an information rich small molecule, in which programable rotational speed states can be observed with facile read-out (fluorescence or ^{1}H NMR spectroscopy) and should pave the way for the development of more sensitive fluorescent thermometers for a desired temperature range. Ideally, such systems would provide a ratiometric response or display changes in fluorescence lifetime upon binding rather than relying on changes in emission intensity at a single wavelength. Future work will focus on the development of molecules with these properties.

Supporting Information

Synthetic procedures; copies of the ^{1}H, ^{13}C NMR and HRMS spectra of all novel compounds; fluorescence data; UV-Vis binding studies and fitted titration data; ^{1}H NMR variable temperature and binding studies and fitted titration data; details of the crystal structure determinations of CarROT. Deposition numbers 2076008 and 2076009 (both for CarROT) contain the supplementary crystallographic data for this paper. These data are provided free of charge by the joint Cambridge Crystallographic Data Centre and Fachinformationszentrum Karlsruhe Access Structures service http://www.ccdc.cam.ac.uk/structures. The authors have cited additional references within the Supporting Information.[63–67]

Acknowledgements

This work was supported by the Australian Research Council (DP170100118 to K.A.J.) and was facilitated by access to Sydney Analytical, a core research facility at the University of Sydney. Open Access publishing facilitated by The University of Sydney, as part of the Wiley - The University of Sydney agreement via the Council of Australian University Librarians.

Conflict of Interests

The authors declare no conflict of interest.

Data Availability Statement

The data that support the findings of this study are available from the corresponding author upon reasonable request.

Keywords: macrocycle · fluorescence · rotamers

[1] T. van Leeuwen, A. S. Lubbe, P. Štacko, S. J. Wezenberg, B. L. Feringa, *Nat. Rev .Chem.* **2017**, *1*, 0096.
[2] Y. Tu, F. Peng, X. Sui, Y. Men, P. B. White, J. C. M. van Hest, D. A. Wilson, *Nat. Chem.* **2017**, *9*, 480.
[3] A. Comotti, S. Bracco, P. Valsesia, M. Beretta, P. Sozzani, *Angew. Chem. Int. Ed.* **2010**, *49*, 1760.
[4] A. Comotti, S. Bracco, T. Ben, S. Qiu, P. Sozzani, *Angew. Chem. Int. Ed.* **2014**, *53*, 1043.
[5] M. Inukai, T. Fukushima, Y. Hijikata, N. Ogiwara, S. Horike, S. Kitagawa, *J. Am. Chem. Soc.* **2015**, *137*, 12183.
[6] A. Faulkner, T. van Leeuwen, B. L. Feringa, S. J. Wezenberg, *J. Am. Chem. Soc.* **2016**, *138*, 13597.
[7] G. T. Rushton, E. C. Vik, W. G. Burns, R. D. Rasberry, K. D. Shimizu, *Chem. Commun.* **2017**, *53*, 12469.
[8] Y. Wu, G. Wang, Q. Li, J. Xiang, H. Jiang, Y. Wang, *Nat. Commun.* **2018**, *9*, 1953.
[9] A. Goswami, I. Paul, M. Schmittel, *Chem. Commun.* **2017**, *53*, 5186.
[10] B. E. Dial, P. J. Pellechia, M. D. Smith, K. D. Shimizu, *J. Am. Chem. Soc.* **2012**, *134*, 3675.
[11] S. J. Wezenberg, B. L. Feringa, *Nat. Commun.* **2018**, *9*, 1984.
[12] T. Hirao, D. S. Kim, X. Chi, V. M. Lynch, K. Ohara, J. S. Park, K. Yamaguchi, J. L. Sessler, *Nat. Commun.* **2018**, *9*, 823.
[13] G. Wang, H. Xiao, J. He, J. Xiang, Y. Wang, X. Chen, Y. Che, H. Jiang, *J. Org. Chem.* **2016**, *81*, 3364.

[14] S. K. Samanta, M. Schmittel, *J. Am. Chem. Soc.* **2013**, *135*, 18794.
[15] R. Schettini, C. Costabile, G. Della Sala, V. Iuliano, C. Tedesco, I. Izzo, F. De Riccardis, *J. Org. Chem.* **2018**, *83*, 12648.
[16] M. S. Özer, I. Paul, A. Goswami, M. Schmittel, *Dalton Trans.* **2019**, *48*, 9043.
[17] P. C. Knipe, S. Thompson, A. D. Hamilton, *Chem. Sci.* **2015**, *6*, 1630.
[18] T. Qin, B. Liu, K. Zhu, Z. Luo, Y. Huang, C. Pan, L. Wang, *TrAC Trends Anal. Chem.* **2018**, *102*, 259.
[19] X. D. Wang, O. S. Wolfbeis, R. J. Meier, *Chem. Soc. Rev.* **2013**, *42*, 7834.
[20] G. B. Kauffman, S. Uchiyama, A. P. Silva, *J. Chem. Educ.* **2006**, *83*, 720.
[21] G. S. Kottas, L. I. Clarke, D. Horinek, J. Michl, *Chem. Rev.* **2005**, *105*, 1281.
[22] Z. Yang, J. Cao, Y. He, J. H. Yang, T. Kim, X. Peng, J. S. Kim, *Chem. Soc. Rev.* **2014**, *43*, 4563.
[23] Y. Takei, S. Arai, A. Murata, M. Takabayashi, K. Oyama, S. Ishiwata, S. Takeoka, M. Suzuki, *ACS Nano* **2014**, *8*, 198.
[24] C. D. S. Brites, P. P. Lima, N. J. O. Silva, A. Millán, V. S. Amaral, F. Palacio, L. D. Carlos, *Nanoscale* **2012**, *4*, 4799.
[25] G. Liebsch, I. Klimant, O. S. Wolfbeis, *Adv. Mater.* **1999**, *11*, 1296.
[26] T. Plakhotnik, M. W. Doherty, J. H. Cole, R. Chapman, N. B. Manson, *Nano Lett.* **2014**, *14*, 4989.
[27] Feng, K. Tian, D. Hu, S. Wang, S. Li, Y. Zeng, Y. Li, G. Yang, *Angew. Chem. Int. Ed.* **2011**, *50*, 8072.
[28] D. Su, C. L. Teoh, L. Wang, X. Liu, Y. T. Chang, *Chem. Soc. Rev.* **2017**, *46*, 4833.
[29] M. S. A. Abdel-Mottaleb, R. O. Loutfy, R. Lapouyade, *J. Photochem. Photobiol. A* **1989**, *48*, 87.
[30] Q. Fang, J. Li, S. Li, R. Duan, S. Wang, Y. Yi, X. Guo, Y. Qian, W. Huang, G. Yang, *Chem. Commun.* **2017**, *53*, 5702.
[31] Y. Wu, J. Liu, Y. Wang, K. Li, L. Li, J. Xu, D. Wu, *ACS Appl. Mater. Interfaces* **2017**, *9*, 11073.
[32] S. Uchiyama, Y. Matsumura, A. P. de Silva, K. Iwai, *Anal. Chem.* **2003**, *75*, 5926.
[33] B. Bardi, I. Tosi, F. Faroldi, L. Baldini, F. Sansone, C. Sissa, F. Terenziani, *Chem. Commun.* **2019**, *55*, 8098.
[34] S. Liang, Y. Wang, X. Wu, M. Chen, L. Mu, G. She, W. Shi, *Chem. Commun.* **2019**, *55*, 3509.
[35] J. H. Tang, Y. Sun, Z. L. Gong, Z. Y. Li, Z. Zhou, H. Wang, X. Li, M. L. Saha, Y. W. Zhong, P. J. Stang, *J. Am. Chem. Soc.* **2018**, *140*, 7723.
[36] A. Vyšniauskas, M. Qurashi, N. Gallop, M. Balaz, H. L. Anderson, M. K. Kuimova, *Chem. Sci.* **2015**, *6*, 5773.
[37] T. Xia, L. Wang, Y. Qu, Y. Rui, J. Cao, Y. Hu, J. Yang, J. Wu, J. Xu, *J. Mater. Chem. C* **2016**, *4*, 5696.
[38] M. Homma, Y. Takei, A. Murata, T. Inoue, S. Takeoka, *Chem. Commun.* **2015**, *51*, 6194.
[39] K. Li, Y. Liu, Y. Li, Q. Feng, H. Hou, B. Z. Tang, *Chem. Sci.* **2017**, *8*, 7258.
[40] J. Yu, L. Sun, H. Peng, M. I. J. Stich, *J. Mater. Chem.* **2010**, *20*, 6975.
[41] H. S. Peng, S. H. Huang, O. S. Wolfbeis, *J. Nanopart. Res.* **2010**, *12*, 2729.
[42] A. Tsuda, S. Sakamoto, K. Yamaguchi, T. Aida, *J. Am. Chem. Soc.* **2003**, *125*, 15722.
[43] E. J. McLaurin, V. A. Vlaskin, D. R. Gamelin, *J. Am. Chem. Soc.* **2011**, *133*, 14978.
[44] L. Lu, G. Yang, Y. Xia, *Anal. Chem.* **2014**, *86*, 6188.
[45] L. M. Maestro, E. M. Rodríguez, F. S. Rodríguez, M. C. I. De La Cruz, A. Juarranz, R. Naccache, F. Vetrone, D. Jaque, J. A. Capobianco, J. G. Solé, *Nano Lett.* **2010**, *10*, 5109.
[46] Y. Shiraishi, R. Miyamoto, T. Hirai, *Langmuir* **2008**, *24*, 4273.
[47] K. Okabe, N. Inada, C. Gota, Y. Harada, T. Funatsu, S. Uchiyama, *Nat. Commun.* **2012**, *3*, 705.
[48] C. Y. Chen, C. T. Chen, *Chem. Commun.* **2011**, *47*, 994.
[49] S. Arai, M. Suzuki, S. J. Park, J. S. Yoo, L. Wang, N. Y. Kang, H. H. Ha, Y. T. Chang, *Chem. Commun.* **2015**, *51*, 8044.
[50] S. Arai, S. C. Lee, D. Zhai, M. Suzuki, Y. T. Chang, *Sci. Rep.* **2014**, *4*, 6701.
[51] Y. Ni, M. E. Sandoval-Salinas, T. Tanaka, H. Phan, T. S. Herng, T. Y. Gopalakrishna, J. Ding, A. Osuka, D. Casanova, J. Wu, *Chem* **2019**, *5*, 108.
[52] I. Alfonso, M. I. Burguete, S. V. Luis, *J. Org. Chem.* **2006**, *71*, 2242.
[53] S. Pulacchini, R. Nasser, K. F. Sibbons, M. Motevalli, G. E. Hawkes, R. T. Kroemer, E. S. Bento, M. Watkinson, *Org. Biomol. Chem.* **2003**, *1*, 4058.
[54] L. L. Tian, C. Wang, S. Dawn, M. D. Smith, J. A. Krause, L. S. Shimizu, *J. Am. Chem. Soc.* **2009**, *131*, 17620–17629.
[55] S. N. Berry, L. Qin, W. Lewis, K. A. Jolliffe, *Chem. Sci.* **2020**, *11*, 7015.
[56] F. Gasparro, N. Kolodny, *J. Chem. Educ.* **1977**, *54*, 258.
[57] L. Belvisi, C. Gennari, A. Mielgo, D. Potenza, C. Scolastico, *Eur. J. Org. Chem.* **1999**, 389.
[58] http://www.supramolecular.org (accessed: January 2019).
[59] P. A. Gale, *Chem. Commun.* **2008**, 4525.
[60] F. G. Bordwell, X. Zhang, J. P. Cheng, *J. Org. Chem.* **1991**, *56*, 3216.
[61] V. Almendola, D. Esteban-Gómez, L. Fabbrizzi, M. Licchelli, E. Monzani, F. Sancenón, *Inorg. Chem.* **2005**, *44*, 8690.
[62] G. Canudo-Barreras, L. Ortego, A. Izaga, I. Marzo, R. P. Herrera, M. Concepción Gimeno, *Molecules* **2021**, *26*, 6891.
[63] L. Qin, S. J. N. Vervuurt, R. B. P. Elmes, S. N. Berry, N. Proshogo, K. A. Jolliffe, *Chem. Sci.* **2020**, *11*, 201.
[64] O. V. Dolomanov, L. J. Bourhis, R. J. Gildea, J. A. K. Howard, H. Puschmann, *J. Appl. Crystallogr.* **2009**, *42*, 339.
[65] L. J. Bourhis, O. V. Dolomanov, R. J. Gildea, J. A. K. Howard, H. Puschmann, *Acta Crystallogr. Sect. A Found. Crystallogr.* **2015**, *71*, 59.
[66] G. M. Sheldrick, *Acta Crystallogr. Sect. C Struct. Chem.* **2015**, *71*, 3.
[67] Bruker Inc., VT Calibration Manual, Bruker BioSpin Ag, Switzerland, **2012**.

Manuscript received: February 4, 2024
Accepted manuscript online: March 18, 2024
Version of record online: ■■, ■■

RESEARCH ARTICLE

The molecular motion of macrocyclic carbazole macrocycles (CarROTs) is controlled through the external addition of anions, cations or through deprotonation allowing four discreet rotational speeds to be accessed, which in turn stop, reduce or enhance the thermoluminescent properties due to increasing or decreasing non-radiative decay processes, thereby providing a means to externally control the temperature sensitivity of the system.

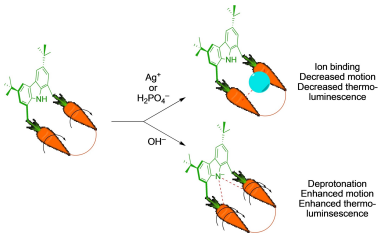

*Dr. S. N. Berry, M. Zou, S. L. Nguyen, A. E. Sajowitz, Dr. L. Qin, Dr. W. Lewis, Prof. K. A. Jolliffe**

1 – 10

Supramolecular Control of the Temperature Responsiveness of Fluorescent Macrocyclic Molecular Rotamers